

SPECTROSCOPY OF ATOMS AND MOLECULES

Optimization of Sub-Doppler Absorption Contour in Gas-Dynamic Beams

M. Yu. Zakharov^a, N. N. Bezuglov^a, N. M. Lisenkov^a, A. N. Klyucharev^a,
I. I. Beterov^b, K. Michulis^c, A. Ékers^c, F. Fuso^d, and M. Allegrini^d

^a St. Petersburg State University, Peterhof, St. Petersburg, 198504 Russia

^b Institute of Semiconductor Physics, Siberian Branch, Russian Academy of Sciences, Novosibirsk, 630090 Russia

^c Laser Center, University of Latvia, LV-1002 Riga, Latvia

^d Dipartimento di Fisica Enrico Fermi and CNISM, Università di Pisa, I-56127 Pisa, Italy

Received October 8, 2009

Abstract—The formation of the Doppler contour $P_D(v)$ of absorption lines upon the excitation of particles in the volume of a gas-dynamic beam by light propagating in a direction orthogonal (reduced) to the beam axis is analyzed. Integral representations of $P_D(v)$ are obtained for arbitrary relations between the nozzle outlet diameter D and the collimating aperture diameter B in the excitation region are obtained. An optimal configuration at which the reduced Doppler contour is the narrowest at a high density of beam particles is revealed to be $B/D = 2$.

DOI: 10.1134/S0030400X10060093

INTRODUCTION

Atomic/molecular beams have been widely used in practice as convenient sources of particles, which make it possible to perform investigations in the physics of collisions, spectroscopy, and the analysis of the interaction of light and matter [1]. Among the applied fields, one should single out atomic lithography where specified spatial structures are formed from beam particles using masks. In the recent decades, a new type of beam known as “cold beams” has been added to the two classical types of beams, i.e., diffusion and gas-dynamic [2–4]. These beams have unique prospects for use in nanotechnology [5] due to their extremely narrow divergence angle. The production of cold beams is based on the pyramidal configuration of a magneto-optical trap for atomic Cs. An experimental setup [4] consists of a four-chamber high-vacuum system that contains prisms and mirrors in a pyramidal configuration. The setup ensures either a static magneto-optical trap with a high density of atoms or a laser-cooled continuous beam of cold atoms due to the use of six independent laser diode systems in a master-oscillator configuration. The original production of a laser-cooled beam of Cs atoms [4] combines subthermal properties (longitudinal and transverse velocities of 10 and 1 cm/s, respectively) at a relatively large particle density (more than 10^{11} cm⁻³). These parameters of the beam are also of great interest in studies of chemoionization reactions involving the participation of Rydberg atoms. As was shown in the cycle of studies [6–8], subthermal conditions with respect to the relative impact velocity prove to be favorable for the devel-

opment and observation of the dynamic chaos regime for orbits of a Rydberg electron in quasi-molecular collisional complexes.

The obvious limitations of cold beams are related to the small number of atoms that can be laser-cooled, as well as the impossibility of working with molecules. Therefore, the most universal type of beams are gas-dynamic beams, which, unlike diffusion beams, ensure comparatively small relative dispersion of velocities of beam particles. For atoms and molecules in the gas phase, the corresponding effective temperature can be reduced to about 10 K by creating a fairly large pressure difference before and after the nozzle. For particles whose gas states are formed at high temperatures, the pressure is not restricted by the saturation vapor pressure; therefore, the velocity dispersion is related to the type of atomic/molecular particles. Thus, for the sodium atom and scheme of the gas-dynamic beam presented in Fig. 1, typical mass (average) velocity v_f is ~ 1000 m/s, whereas the spread of velocities v_T relative to the mass velocity is ~ 200 m/s [9, 10].

A feature of gas-dynamic beams that is important for practice is that absorption contours are very narrow (sub-Doppler), which is related with a unidirectional character of motion of particles along the beam axis z and their collimation with skimmers and aperture B (Fig. 1). The narrowing of spectral lines is maximal if the direction of propagation of photons is orthogonal (reduced) to the direction of propagation of the gas-dynamic beam. The finite, nonzero, collimation angle $\varphi = B/L$ gives rise to the reduced Doppler width

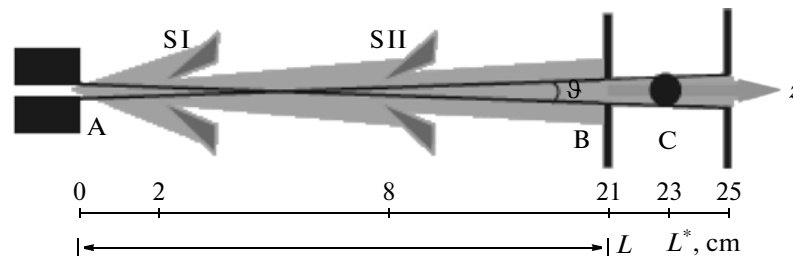


Fig. 1. Collimation scheme of atomic beam using skimmers and diaphragm. Excitation region C of atoms (dark spot) and diaphragm B (diameter $B = 2$ mm) are at distances $L^* = 23$ cm and $L = 21$ cm, respectively, from nozzle outlet A (diameter $D = 0.4$ mm), SI and SII are skimmers (diameters $D_1 = 2$ mm, $D_2 = 1.5$ mm).

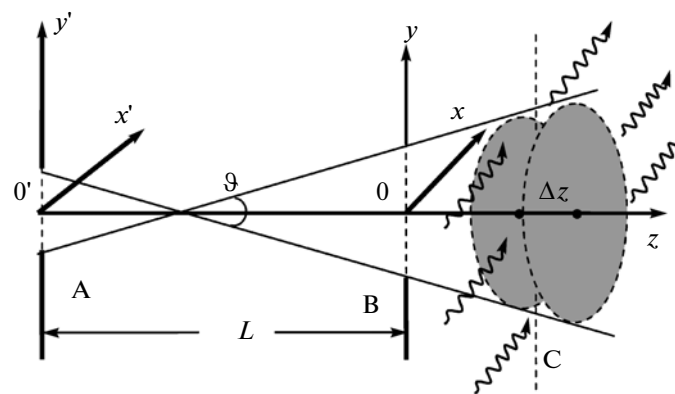


Fig. 2. Simplified (without skimmers) geometry of atomic beam. Excitation zone C is a cylinder with a radius $R = L^* \vartheta / 2 - D/2$ and thickness Δz .

$\Delta v_D \approx v_f / \lambda \sin \varphi$, where λ is the wavelength of the line. For typical experimental parameters [10] ($\lambda \approx 5890 \text{ \AA}$, $v_f \approx 1200$ m/s, $\varphi \approx 1^\circ$) $\Delta v_D \approx 36$ MHz, which considerably exceeds the natural width $\Delta v_{\text{nat}} = 1/(\tau_{\text{nat}} 4\pi) = 4.9$ MHz of the resonance line of the sodium atom. In principle, the collimation angle can be simply reduced by decreasing the diameter B of diaphragm B with the distance L being fixed; however, in the experiment, this is restricted by two factors, including (i) the number of particles in the excitation region decreases and (ii) particles condense on the material of the diaphragm. The latter circumstance makes it impossible, e.g., to work for a long period of time with diameters $B < 2$ mm in the configuration of Fig. 1 [10] because settling sodium rather rapidly (anywhere from dozens of minutes to a few hours depending on the beam intensity) plugs the diaphragm hole.

This paper reports on the rather surprising possibility of narrowing the widths of reduced Doppler contours $P_D(v)$ by increasing the nozzle outlet, with the dimensions of the collimating aperture remaining unchanged. We note that, in our previous work [11],

which was devoted to particular features of $P_D(v)$ in diffusion and gas-dynamic beams, the nozzle diameter was assumed to be negligibly small compared to all other dimensions indicated in Fig. 1.

REDUCED DOPPLER PROFILE

Doppler contours of lines $P_D(v)$ detected in the laboratory coordinate system are formed because of dipolar shifts of photons emitted or absorbed by moving particles (atoms or molecules). In a gas cell, the contour $P_D(v)$ has a Gaussian shape because the velocity distribution of particles in the cell is Maxwellian (thermal). The central part (core) of the reduced contour $P_D(v)$ of the gas-dynamic beam in the direction perpendicular to the beam axis differs from an exponential function because its formation is mainly determined by the distribution of particles over their exit angle within the collimation angle, i.e., is determined by the geometry of the beam [11].

PARAMETERS OF GAS-DYNAMIC BEAM

The collimation scheme and the geometry of a gas-dynamic beam are presented in Figs. 1, 2. Due to heating in an effusion source, atoms or molecules of the beam are prepared in the gas phase at a temperature \tilde{T} and, through the nozzle outlet A, after expansion, are directed into the reaction zone C, which is located at a distance L^* from the outlet A. The beam formation scheme, which consists of two skimmers and diaphragm B, cuts a narrow solid angle with an opening ϑ (the collimation angle). We note that the skimmers cut an angle larger than ϑ and decrease the mass of particles, which are settled on the diaphragm. The skimmers also separate chambers with different degrees of differential pumping. Upon consideration of the geometry of the gas-dynamic beam (Fig. 2), they can be neglected. In this work, we do not impose significant restrictions on the size of elements of the gas-dynamic beam (except for the requirement of smallness of the angle ϑ) and adopt the following natural assumptions concerning the spatial (angular) distribution of beam particles:

(i) The collimation angle $\vartheta = (D + B)/L$ is assumed to be small ($\sim 1^\circ$).

(ii) The flux density of particles leaving the nozzle is assumed to be homogeneous along the surface of the outlet A.

(iii) The angular distribution of particles within the narrow solid angle with the opening ϑ is assumed to be isotropic with respect to the exit angle.

(iv) Using cylindrical focusing lenses [10, 12], the spatial size of the laser beam in the excitation zone C exceeds its radius $R = L^* \vartheta/2 - D/2$ (Fig. 2). This means that the photon flux $I(z)$ completely covers the atomic beam in the zone C and is homogeneously distributed over coordinates $\{x, y\}$.

(v) The radiation intensity distribution $I(z) = I_0 \exp(-2(z - L^*)^2/\Delta z^2)$ along the beam axis is described by a Gaussian function with a width Δz [12]. The magnitude of Δz is determined by the focusing of the laser beam and specifies the thickness of the excitation zone C, which assumed to be small compared to the distance L^* to the source A. This allows us to consider the spatial distribution of beam particles to be homogeneous in the volume C.

The assumptions allow us to simply describe the direction \mathbf{n} of a rectilinear trajectory of a particle that leaves plane A at point \mathbf{r}' and intersects the plane of the diaphragm B at point \mathbf{r} as follows:

$$\mathbf{n} = \frac{\mathbf{r} - \mathbf{r}'}{|\mathbf{r} - \mathbf{r}'|} = \frac{\mathbf{r} - \mathbf{r}'}{L} \quad (1)$$

The equality $|\mathbf{r} - \mathbf{r}'| = L$ follows from the smallness of the angular dimensions of the holes A and B. In calculations of the contour $P_D(\nu)$, we are interested in the

velocity of particles $\mathbf{v} = \nu \mathbf{n}$ that enter into the relation for the Doppler shift $\Delta \nu_D = \mathbf{\Omega} \mathbf{v} / \lambda$, where $\mathbf{\Omega}$ is the direction of propagation of a photon with a wavelength λ . In the case of gas-dynamic beams, the distribution $F(\nu)$ normalized over the absolute value of the velocity ν is determined by the Maxwellian distribution function [1–3]

$$F_{GD}(\nu) = \frac{\nu^2}{\sqrt{\pi} \nu_f \nu_T} \exp\left(-\frac{(\nu - \nu_f)^2}{\nu_T^2}\right) \quad (2)$$

The characteristic velocity dispersion ν_T is specified by the expansion (cooling) of the gas jet in the nozzle of the gas-dynamic beam, with its typical value being $\nu_T \sim 200$ m/s. In this case, the mass velocity becomes the average velocity of motion of particles of the gas-dynamic beam, with the value of this parameter being ~ 1000 m/s [9].

INTEGRAL REPRESENTATION
FOR $P_D(\nu)$

Let a gas-dynamic beam be excited by light from a monochromatic laser beam whose frequency is ν and the detuning from the line center is $\Delta \nu = \nu - \nu_0$. Light quanta are directed perpendicular to the beam axis (z axis with a unit vector \mathbf{e}_z) along the x axis to the excitation region C (Fig. 2); i.e., direction $\mathbf{\Omega}$ coincides with the unit vector \mathbf{e}_x . By definition, the reduced Doppler absorption profile $P_D(\nu)$ is the probability $P(\Delta \nu) d\Delta \nu$ of detecting a beam particle in the excitation volume, with the Doppler shift of the particle $\Delta \nu_D = \mathbf{n} \mathbf{e}_x \nu / \lambda = \mathbf{n}_x \nu / \lambda$ being in the frequency interval $(\Delta \nu, \Delta \nu + d\Delta \nu)$. Because $\Delta \nu_D$ depends on only on the projection \mathbf{n}_x of direction (1) onto the x axis, all particles that move along the same trajectory at the same velocity ν will make equal contributions to the sought probability. In other words, we are interested in the relative weight $P(\Delta \nu)$ of trajectories, which is in no way related to the z coordinate. The particle trajectories are uniquely parameterized by the previously introduced coordinates \mathbf{r}' on the plane A and coordinates \mathbf{r} on the plane B. It is convenient to count the position of the vector \mathbf{r} from the new coordinate origin 0 placed at the center of the diaphragm B (in this case, the previous coordinate origin 0' of the vector \mathbf{r}' , which is located at the center of the nozzle outlet, remains the same). The shift $\Delta \nu_D$ can now be easily represented as $\Delta \nu_D = (\mathbf{r} + L \mathbf{e}_z - \mathbf{r}')_x \nu / L \lambda =$

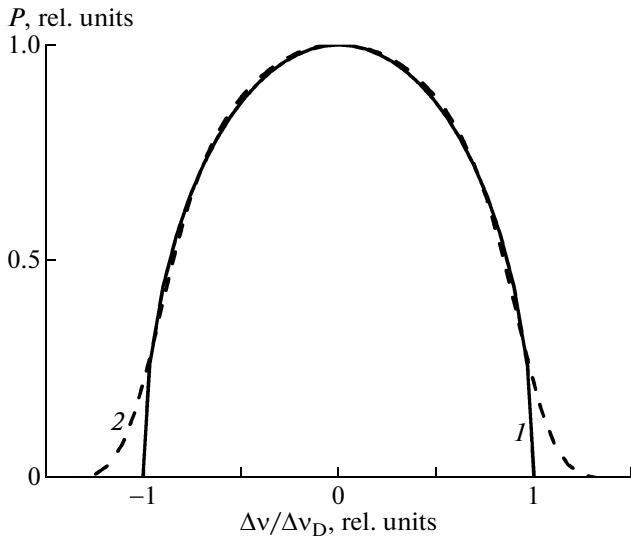


Fig. 3. Profile $P_D(v)$ normalized to unity at the line center in the case $D \ll B$: (1) core, formulas (4) and (7); (2) exact profile, formula (3).

$(x - x')v/L\lambda$ so that the normalized probability $P(\Delta v)$ takes the form

$$P_D(v) = P(\Delta v) = \frac{16}{\pi^2 D^2 B^2} \iint_{\pi D^2/4} dy' dx' \iint_{\pi B^2/4} dy dx \int_0^\infty dv F_{GD}(v) \times \delta(\Delta v - (x - x')v/L\lambda). \quad (3)$$

The double integral over the surfaces of the nozzle outlet and diaphragm sums the probabilities of trajectories that pass through the points $(x'y')$ and (xy) , whereas the integral over velocities takes into account the velocity distribution. By virtue of the spatial homogeneity of beam particles, particles equiprobably intersect the planes A and B. The one-dimensional Dirac function δ cuts from all trajectories only those that match the Doppler shift Δv_D of moving particles and the laser detuning Δv .

ANALYSIS OF PARTICULAR FEATURES OF PROFILE $P_D(v)$

Relation (3) is the exact integral representation for the reduced Doppler contour $P_D(v)$. The probability $P(\Delta v)$ is normalized to unity, i.e., $\int d(\Delta v) P(\Delta v) = 1$. In this work, we are mainly interested in analysis of the width Δv_{HWHM} (halfwidth at half maximum) of the contour $P_D(v)$. Based on the results of [11], it can be shown that, because the large parameter $\Lambda = v_f/v_T \approx 5$ exists, the velocity distribution $F_{GD}(v)$ (2) is only responsible for the formation of relatively

far wings. The central part (core) $\tilde{P}(\Delta v)$ of the absorption contour $P_D(v)$ can be found with a high accuracy assuming that the modulus of the velocity remains unchanged, $v \equiv v_f$,

$$\tilde{P}(\Delta v) = \frac{16}{\pi^2 D^2 B^2} \iint_{\pi D^2/4} dy' dx' \times \iint_{\pi B^2/4} dy dx \delta(\Delta v - (x - x')v_f/L\lambda). \quad (4)$$

Figure 3 compares the behavior of the core $\tilde{P}(\Delta v)$ of the profile (curve 1) calculated by representation (4) (see also formula (7) below) with the behavior of the profile $P(\Delta v)$ found from exact expression (3) in the case of the point source of the gas-dynamic beam using the method described in [11].

CORE OF THE PROFILE $P_D(v)$

It can be seen from Fig. 3 that, in order to find the width Δv_{HWHM} , it is sufficient to restrict oneself to the analysis of the core of profile (4), which, after standard transformations, can be further simplified taking into account the fact that the simplicity of the dependence of the integrand on the difference $x - x'$ as follows:

$$\tilde{P}(\Delta v) = \frac{1}{\Delta v_D \pi a^2} \int_{-a}^a dx' \sqrt{a^2 - x'^2} \times \int_{-1}^1 dx \sqrt{1 - x^2} \delta(\Delta v/\Delta v_D - x - x'); \quad (5)$$

$$a = D/B; \quad \Delta v_D = \varphi v_f/\lambda; \quad \varphi = 0.5B/L. \quad (6)$$

Here, the quantity Δv_D acts as a characteristic reduced Doppler width. As follows from (6), it gives the Doppler shift for particles such that having begun to move from the center O' of the nozzle outlet touch the edge of the diaphragm hole. Note that, in fact, the double integral in (5) is reduced to a single integral because of the presence of the δ -function.

Assuming that the ratio $a = D/B$ is small (the nozzle outlet is relatively small), we can equate to zero the coordinate x' in the argument of δ -function (5); as a result, integral (5) can be represented by the simple expression

$$\tilde{P}(\Delta v) = \frac{1}{\Delta v_D \pi} \sqrt{1 - \frac{\Delta v^2}{\Delta v_D^2}}; \quad D \ll B, \quad (7)$$

which describes the behavior of curve 1 in Fig. 3.

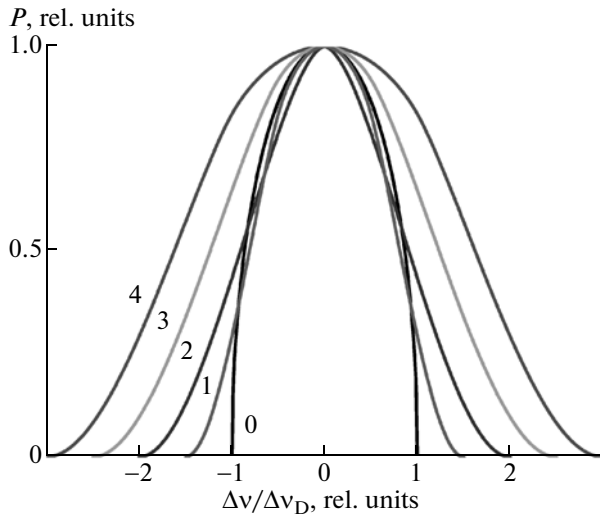


Fig. 4. Profiles of reduced absorption contour normalized to unity at line center calculated for nozzle outlet diameter $D = 0, 1, 2, 3,$ and 4 mm. Diameter of diaphragm is $B = 2$ mm.

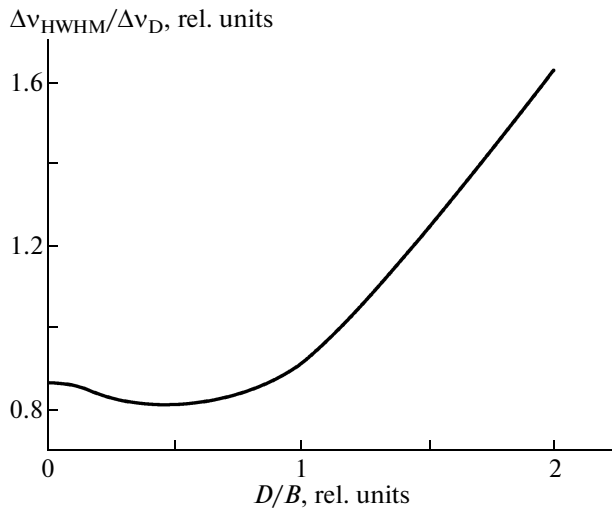


Fig. 5. HWHM Δv_{HWHM} of reduced Doppler profile in units of Δv_D as a function of nozzle outlet diameter D (in units of diameter of diaphragm). In calculations, diameter of diaphragm B was taken to be 2 mm.

HALFWIDTH Δv_{HWHM} OF THE PROFILE $P_D(v)$

Figure 4 presents results calculations of the central part of the reduced Doppler absorption profile for different values of the diameter D of the nozzle outlet. The diameter of the diaphragm is fixed to be $B = 2$ mm, with this value being taken from the scheme of the experimental setup in Fig. 1. We note two characteristic features in the behavior of the profiles. (i) The

light absorption turns to zero at $|\Delta v| \geq (1 + D/L)\Delta v_D$. This property follows from the assumption that the mass velocity is the same for all beam particles, which underlies expression (5). Indeed, the maximal possible angle of the deviation of particle trajectory from the beam axis is restricted by the collimation angle $\vartheta = (D + B)/L$ (Figs. 1, 2). Consequently, the Doppler shift cannot exceed the quantity $0.5\theta v_f/\lambda = (1 + D/L)\Delta v_D$, and light with a greater detuning has no effect on beam particles. A relatively small (20%) spread in velocities around v_f somewhat spreads (also at a level of 20%) this ultimate value (Fig. 3), but hardly affects the behavior of the main part of the contour at all. (ii) An unexpected peculiarity in the behavior of the curves of Fig. 4 is related to the monotonic decrease in their halfwidth Δv_{HWHM} with increasing nozzle size in the range $D < B/2$. Note that, outside of their halfwidth (i.e., in wings), profiles nevertheless show a tendency to broaden.

CONCLUSIONS

The accuracy of the extraction of useful information from experimental data depends to a large extent on how fully the relevant instrumental function is known. In interpretation of absorption or fluorescence spectra, among important factors of formation of accompanying instrumental functions are particular mechanisms of broadening of spectral lines, which can, e.g., substantially distort intensity ratios between hyperfine structure components in absorption spectra of resonance lines of alkali metals [9, 10]. This work continues the investigations of [11] of the behavior of the reduced Doppler absorption contour $P_D(v)$ caused by the divergence of the gas-dynamic beam at a finite collimation angle $\vartheta = (D + B)/L$. This angle is the sum of the two terms, D/L and B/L , each of which is determined by the apertures of the nozzle outlet and collimating diaphragm (Figs. 1, 2). The results of this work indicate that there is a paradoxical possibility of reducing the halfwidth of the profile Δv_{HWHM} by increasing the collimation angle ϑ , more exactly, its part D/L , which is related with the aperture of the nozzle outlet (Fig. 5). The advantage of this optimization of the contour $P_D(v)$ consists of a simultaneous increase in the density of beam particles.

ACKNOWLEDGMENTS

This work was supported by the Russian Foundation for Basic Research (RFBR) (project no. 09-02-92428-KÉ_a) within the framework of the bilateral EINSTEIN CONSORTIUM/RFBR project “Non-linear Dynamic Resonances at Collective Interactions of Cold Atoms,” by the European Program EU FP7 IRSES Project COLIMA, and by the Latvian Science Council.

REFERENCES

1. *Atomic and Molecular Beam Techniques*, Ed. by G. Scoles (Oxford Univ. Press, Oxford, 1988).
2. V. B. Leonas, *Usp. Fiz. Nauk* **27**, 319 (1979).
3. N. F. Ramsey, *Molecular Beams*, 2nd ed. (Clarendon, Oxford, 1989).
4. A. Camposeo et al., *Opt. Commun.* **200**, 231 (2001).
5. C. O'dwyer, G. Gay, B. Viaris de Lesegno, et al., *Nanotechnology* **16**, 1536 (2005).
6. N. N. Bezuglov, V. M. Borodin, A. N. Klyucharev, et al., *Opt. Spektrosk.* **86** (6), 922 (1999).
7. N. N. Bezuglov, V. M. Borodin, A. Ekers, and A. N. Klyucharev, *Opt. Spektrosk.* **93** (4), 721 (2002).
8. K. Miculis, I. I. Beterov, N. N. Bezuglov, I. I. Ryabtsev, D. B. Tretyakov, A. Ekers, and A. N. Klucharev, *J. Phys. B* **38**, 1811 (2005).
9. R. Garcia-Fernandez, A. Ekers, J. Klavins, L. P. Yatsenko, N. N. Bezuglov, B. W. Shore, and K. Bergmann, *Phys. Rev. A* **71**, 023 401 (2005).
10. I. Sydoryk, N. N. Bezuglov, I. I. Beterov, et al., *Phys. Rev. A* **77**, 042511 (2008).
11. N. N. Bezuglov, M. Zakharov, A. N. Klyucharev, et al., *Opt. Spektrosk.* **102**, 894 (2007).
12. W. Demtröder, *Laser Spectroscopy* (Springer, Berlin, 2003).

Translated by V. Rogovoi